

# Computer Aided Design of Horn Radiators for Satellite Communication by Least Squares Optimization

C. Hartwanger<sup>1</sup>, K. Schittkowski<sup>2</sup>, H. Wolf<sup>3</sup>

## Abstract

Computer aided design optimization of corrugated horns became a powerful tool to reduce development costs on the one hand and to improve performance of space antennas on the other. In this paper the physical model is outlined, based on Maxwell's equations, and it is shown, how a complete numerical simulation of a circular corrugated horn can be achieved, assuming that the interior geometry of the horn is known. In order to compute the electromagnetic properties of a horn, the so-called scattering matrix is assembled. This matrix is needed to relate mode amplitudes of reflected and transmitted waves in horn sections with different diameters. Envelope functions, determined by a few geometric design parameters, are used to describe the inner geometry of a horn. These parameters are applied to formulate a least squares optimization problem. As a starting point, an amplitude spectrum in the aperture has to be determined which radiates a given far field. The differences of those amplitudes and the amplitudes predicted by the model are to become as small as possible by adapting the design variables. Moreover, the return loss is to be minimized. The resulting least squares optimization problem can

---

<sup>1</sup>Institute of Radio Frequency Technology, German Aerospace Center, 82234 Wessling, Germany

<sup>2</sup>Department of Mathematics, University of Bayreuth, 95440 Bayreuth, Germany

<sup>3</sup>Dornier Satellite Systems Ltd., Antennas and Payload Components, 81663 München, Germany

be solved by a standard sequential quadratic programming (SQP) code after a suitable transformation into a nonlinear programming problem, by which typical features of Gauss-Newton methods are retained. Some numerical results are included to show the successfull application of the introduced advance to design a circular corrugated horn which radiates a given far field.

*Keywords:* Antenna design; corrugated horns; wave equation; least squares optimization

## 1 Introduction

Corrugated horns are frequently used as reflector feed sources for large space antennas, e.g. for INTELSAT satellites, see Wolf et al. [33].

The goal is, to achieve a given spatial energy distribution of the radio frequency (RF) waves, called the radiation or directional characteristic. The transmission quality of the information, carried by the RF signals, is strongly determined by the directional characteristic of the feeding horn, i.e. it's geometric structure.

Today, the experimental design of corrugated horns, based on a trial-and-error approach, is replaced by a computer aided design, where the dynamic system is modeled completely in a mathematically rigorous way, see Kühn and Hombach [15] for horns with ring-loaded radial slots, or Cocciali et al. [3], Clarricoats, Olver [2] and Olver et al. [24], [23] for alternative horn types.

Another drastic improvement in the design process was achieved by applying nonlinear programming techniques. Optimization variables describe completely the interior horn geometry, e.g. length, aperture diameter, wave guide interface, mass, slot width of corrugations, wall thickness, etc. They are iterated by an optimization algorithm with the intention to minimize return loss, cross-polar peak over a specified field of view, the copolar edge tapering at a specified pattern angle, or some other objectives, cf. e.g. Wolf et al. [33], Shee and Smith [29], or the paper of Gentili et al. [8] with some additional information about software. Manufacturing and physical constraints must be taken into account.

The mathematical model is based on Maxwell's equations for electric and magnetic fields, see e.g. Harrington [11]. Because of additional assumptions, e.g., homogeneous and isotropic media, rotational symmetry, and ideal conductivity, it is possible to solve the wave equation analytically and to evaluate electric and magnetic fields in a wave guide by their eigenmodes forming a complete orthogonal system.

However, the model becomes more complex because of the continuous transition between two neighbouring wave guides with different cross sectional areas. The relationship between reflected and transmitted amplitudes in both wave guides is described by a so-called scattering matrix, which has to be computed separately for each horn module conjunction. By successive matrix multiplications, the scattering matrix for the complete transition of the amplitudes at the horn entry and the aperture can be evaluated.

Once the scattering matrix is computed, the sum of the squared differences between the actually computed wave amplitudes and the required ones is evaluated as for the objective function to be minimized. Design parameters, needed for describing the interior horn geometry, are the optimization variables to be adapted in an iterative way.

Least squares problems are solved iteratively by Gauss-Newton and related algorithms, to exploit the special mathematical structure as much as possible and to get efficient and reliable methods, see e.g. Björck [1] or Dennis [5].

Because of the highly complex computations required for creating the scattering matrix, the number of iterations must be as low as possible. Since the applied numerical methods require first derivatives, it is necessary to approximate them numerically by a forward difference formula, an additional burden for the numerical complexity of the described approach.

One possibility to solve a least squares problem is, to transform it into a general constrained nonlinear programming problem by introducing additional variables and constraints, see Schittkowski [28], and to solve the modified optimization problem by a sequential quadratic programming (SQP) code, e.g., by NLPQL of Schittkowski [27]. It can be shown that typical features of a Gauss-Newton method are

retained and that the additional variables and constraints do not increase numerical complexity. By combining the evaluation program for the scattering matrix and the least squares optimization code, a powerful tool to solve the underlying design problem is obtained.

Section 2 contains a brief outline of the underlying physical model equations, i.e. Maxwell's equations and the resulting wave equations. The interior geometry of a circular corrugated horn is described in Section 3, which is needed to formulate the design parameters of our model. The essential time consuming part of the numerical model evaluation is the computation of the scattering matrix, by which amplitudes of aperture modes and wave guide modes can be computed from the given excitation. Corresponding formulas, obtained from continuous transmission conditions, are found in Section 4. In Section 5 the least squares optimization problem is formulated and some numerical details giving insight into the computational procedure, are presented. The iterative solution of least squares problems is based on the Gauss-Newton method, which is described in Section 6. Moreover it is shown how the least squares problem is transformed into a general nonlinear programming problem to be solved by a standard SQP algorithm. Finally numerical results are presented, obtained for an existing satellite horn, to validate the described method.

## 2 Physical Model Equations

In the following, a brief outline of the physical equations is given that are used to model the electromagnetic field of horns. For more details see Jackson [13], Mittra and Lee [21] or Zuhrt [34]. It is assumed, that a circular wave guide with constant diameter is given.

The electromagnetic field theory is based on Maxwell's equations, i.e., four differential equations relating the electrical field  $E$ , the magnetic field  $H$ , the electrical displacement  $D$ , and the magnetic induction  $B$  to electrical charge density  $\rho$  and current density  $J$ , see e.g. Collin [4] or Silver [30]. In a general form these equations

are

$$\begin{aligned}
 \nabla \times H &= J + \frac{\partial}{\partial t} D, \\
 \nabla \times E &= -\frac{\partial}{\partial t} B, \\
 \nabla \cdot B &= 0, \\
 \nabla \cdot D &= \rho
 \end{aligned} \tag{1}$$

with the material conditions

$$\begin{aligned}
 D &= \epsilon_0 \epsilon_r E, \\
 B &= \mu_0 \mu_r H,
 \end{aligned} \tag{2}$$

with  $\epsilon_0$ , the dielectric constant,  $\epsilon_r$ , the relative dielectric constant,  $\mu_0$  the permeability and  $\mu_r$ , the relative permeability.

Under some basic assumptions, e.g., homogenous and isotropic media, Maxwell's equations can be transformed into an equivalent system of two coupled equations. They have the form of a wave equation, i.e.,

$$\nabla^2 \Psi - c^2 \frac{\partial^2}{\partial t^2} \Psi = -f(x, t)$$

with displacement  $f(x, t)$  enforcing the wave, and wave velocity  $c$ .  $x$  is the space variable, and  $\Psi$  is to be replaced respectively either by  $E$  or  $H$ .

For circular horns with rotational symmetry, the usage of cylindrical coordinates  $(\rho, \phi, z)$  is advantageous, especially since only waves propagating in  $z$  direction do occur. Thus the scalar wave equation in cylindrical coordinates is given by

$$\frac{1}{\rho} \frac{\partial}{\partial \rho} \left( \rho \frac{\partial \Psi}{\partial \rho} \right) + \frac{1}{\rho^2} \frac{\partial^2 \Psi}{\partial \phi^2} + \frac{\partial^2 \Psi}{\partial z^2} + k^2 \Psi = 0. \tag{3}$$

The constant  $k$  is known as the propagation constant, which is related to the wave length  $\lambda$  by  $k = \frac{2\pi}{\lambda}$ .

By separation of variables the general solution

$$\begin{aligned}
 \Psi = & \left[ c_1 J_\nu \left( \sqrt{k^2 - k_z^2} \rho \right) + c_2 N_\nu \left( \sqrt{k^2 - k_z^2} \rho \right) \right] \\
 & \left[ c_3 \cos \nu \phi + c_4 \sin \nu \phi \right] \left[ c_5 e^{-ik_z z} + c_6 e^{ik_z z} \right],
 \end{aligned} \tag{4}$$

is obtained with cylindrical Bessel and Neumann functions  $J_\nu$  and  $N_\nu$ ,  $\nu = 1, \dots, 6$ , and some arbitrary coefficients  $c_j$ ,  $j = 1, \dots, 6$ , see e.g. Collin [4], Waldron [32] or Unger [31] for more details.

Further assuming that the surface of the wave guide has ideal conductivity, Dirichlet boundary conditions  $\Psi = 0$  for  $\Psi = E$  and Neumann boundary conditions  $\frac{\partial \Psi}{\partial n} = 0$  for  $\Psi = H$  ( $n$  expressing the normal vector to the surface) at the surface, yield the eigenmodes or eigenwaves for the circular wave guide. For the numerical analysis it is essential to understand that the eigenmodes of the wave guide form a complete orthogonal system. As a consequence any electromagnetic field distribution in a circular wave guide can be expanded into a infinite series of eigenfunctions, see Unger [31], Waldron [32]. Therefore, the electromagnetic field in the wave guide is completely described by the amplitudes of the modes.

For the discussed problem only the transversal eigenfunctions of the wave guides need to be considered. The eigenfunctions of the circular wave guide are given in the form

$$T_{np}^H = \sqrt{\frac{2 - \delta_{n0}}{(\bar{x}_{np}^{'2} - n^2)\pi}} \frac{J_n(\bar{x}_{np}^{'\frac{\rho}{z}})}{|J_n(\bar{x}_{np}^{'})|} \begin{cases} \sin n\phi \\ \cos n\phi \end{cases}, \quad (5)$$

$$T_{np}^E = \sqrt{\frac{2 - \delta_{n0}}{\pi}} \frac{J_n(\bar{x}_{np}^{\frac{\rho}{z}})}{\bar{x}_{np} |J_{n-1}(\bar{x}_{np}^{'})|} \begin{cases} \sin n\phi \\ \cos n\phi \end{cases}. \quad (6)$$

Here  $J_n$  denotes the  $n$ -th Bessel function,  $\bar{x}_{np}$  and  $\bar{x}_{np}^{'}$  the  $p$ -th root of the  $n$ -th Bessel function and the  $p$ -te root of the first derivative of the  $n$ -th Bessel function, respectively,  $n = 0, 1, 2, \dots$ ,  $p = 0, 1, 2, \dots$ . For the last term in (5) and (6) either the upper or lower trigonometric function is used.

### 3 Interior Geometry of Circular Corrugated Horns

Basically, the radiated far field pattern of a horn is determined by the field distribution of the waves emitted from the aperture. On the other hand, the aperture field distribution itself is uniquely determined by the excitation in the feeding wave guide and by the interior geometry of the horn. Therefore, assuming a given excitation,

the far field is mainly influenced by the design of the interior geometry of the horn.

Usually the horn is excited by the  $TE_{11}$  mode, which is the fundamental, i.e., first solution of the wave equation in cylindrical coordinates. In order to obtain a rotationally symmetric distribution of the energy density of the field in the horn aperture, a quasi periodical corrugated wall structure according to Figure 1 is assumed, cf. Wolf et al. [33], and Johnson and Jasik [14].

To reduce the number of optimization parameters, the horn geometry is described by a set of envelope functions from which the actual geometric data for ridges and slots can be derived.

Typically, a horn is subdivided into three sections, cf. Figure 2, consisting of an input section, a conical section, and an aperture section. For the input and the aperture section, the interior and outer shape of slots and ridges is approximated by a 2nd-order polynomial, while a linear function is used to describe the conical section. It is assumed that the envelope functions of ridges and slots are parallel in conical and aperture section.

By this simple analytical approach it is possible to approximate any reasonable geometry with sufficient accuracy by the design parameters

- $r_a$  - aperture radius,
- $x_1$  - length of input section,
- $x_{con}$  - length of conical section,
- $x_a$  - total horn length,
- $\alpha$  - semi flare angle of conical section,
- $l_r$  - width of slots,
- $l_s$  - width of ridges,
- $t_1$  - depth of first slot in input section,
- $t_2$  - depth of slots in conical section,

which will become the variables of the optimization model.

At the break points  $x_1$  and  $x_2$ , respectively, the envelope functions must be continuously differentiable, to achieve smooth transitions from one section to the other. The corresponding formulae are easily derived from the assumptions mentioned, and found in Hartwanger [12].

## 4 Computation of the Scattering Matrix

A circular corrugated horn has a modular structure, where each module consists of a step transition between two circular wave guides with different diameters, see Figure 1. First it is shown, how the amplitudes of waves, travelling towards and away from the break point, can be coupled by a so-called scattering matrix. By combining all modules of the horn step by step, the corresponding scattering matrix describing the total transition of amplitudes from the entry point to the aperture can be computed by successive matrix operations, see also Kühn and Hombach [15], Mittra [20] or Piefke [25]. To give an impression of the complexity of the evaluation of the scattering matrix, the basic steps are repeated without trying to be complete.

From Maxwell's equations it follows that the tangential electrical and magnetical field components must be continuous at the interface between two wave guides. This continuity condition is exploited to compute a relation between the mode amplitudes of the excident  $b_{E,j}^k$ ,  $b_{H,j}^k$  and incident  $a_{E,j}^k$ ,  $a_{H,j}^k$  waves in each wave guide of a module, see Figure 3,  $k = 1, 2$ .

Then voltage and current coefficients are defined by

$$\begin{aligned}
 U_{H,j}^k &:= \sqrt{z_{H,j}^k} (a_{H,j}^k + b_{H,j}^k) , \\
 U_{E,j}^k &:= \sqrt{z_{E,j}^k} (a_{E,j}^k + b_{E,j}^k) , \\
 I_{H,j}^k &:= \frac{1}{\sqrt{z_{H,j}^k}} (a_{H,j}^k - b_{H,j}^k) , \\
 I_{E,j}^k &:= \frac{1}{\sqrt{z_{E,j}^k}} (a_{E,j}^k - b_{E,j}^k) ,
 \end{aligned} \tag{7}$$

where  $z_{H,j}^k$  is the  $j$ -th magnetic and  $z_{E,j}^k$  the  $j$ -th electric field impedance,  $k = 1, 2$ .

From the eigenfunctions the tangential fields in both areas are obtained, i.e.,

$$E_k = \sum_{j=1}^{\infty} \left( U_{H,j}^k e_{H,j}^k + U_{E,j}^k e_{E,j}^k \right) ,$$

$$H_k = \sum_{j=1}^{\infty} \left( I_{H,j}^k h_{H,j}^k + I_{E,j}^k h_{E,j}^k \right) ,$$

$k = 1, 2$ , where the tangential field vectors in case of excitation by the  $TE_{11}$  mode are computed from (5) and (6)

$$e_{H,j}^k(\rho, z, \phi) = \begin{pmatrix} -\frac{1}{\rho} \sqrt{\frac{2}{(x_j' - 1)\pi}} \frac{J_1(x_j' \rho/z)}{|J_1(x_j')|} \cos \phi \\ \sqrt{\frac{2}{(x_j' - 1)\pi}} \frac{J_1'(x_j' \rho/z)}{|J_1(x_j')|} \frac{x_j'}{z} \sin \phi \\ 0 \end{pmatrix} ,$$

$$h_{H,j}^k(\rho, z, \phi) = \begin{pmatrix} -\sqrt{\frac{2}{(x_j' - 1)\pi}} \frac{J_1'(x_j' \rho/z)}{|J_1(x_j')|} \frac{x_j'}{z} \sin \phi \\ -\frac{1}{\rho} \sqrt{\frac{2}{(x_j' - 1)\pi}} \frac{J_1(x_j' \rho/z)}{|J_1(x_j')|} \cos \phi \\ 0 \end{pmatrix} ,$$

$$e_{E,j}^k(\rho, z, \phi) = \begin{pmatrix} -\sqrt{\frac{2}{\pi}} \frac{J_1'(x_j \rho/z)}{|J_0(x_j)|} \frac{x_j}{z} \cos \phi \\ \frac{1}{\rho} \sqrt{\frac{2}{\pi}} \frac{J_1(x_j \rho/z)}{|J_0(x_j)|} \sin \phi \\ 0 \end{pmatrix} ,$$

$$h_{E,j}^k(\rho, z, \phi) = \begin{pmatrix} -\frac{1}{\rho} \sqrt{\frac{2}{\pi}} \frac{J_1(x_j \rho/z)}{|J_0(x_j)|} \sin \phi \\ -\sqrt{\frac{2}{\pi}} \frac{J_1'(x_j \rho/z)}{|J_0(x_j)|} \frac{x_j}{z} \cos \phi \\ 0 \end{pmatrix} .$$

Here  $J_0$  and  $J_1$  denote the 0-th and 1-st Bessel functions,  $x_j$  and  $x'_j$  the  $j$ -th root of the 1-st Bessel function and the  $j$ -th root of the first derivative of the 1-st Bessel function, respectively, where  $k = 1, 2$  and  $j = 1, 2, 3, \dots$ .

At the transition between the two wave guides the tangential fields must be continuous. Moreover, boundary conditions must be satisfied, i.e.,  $E_2 = 0$  for  $r_1 \leq r \leq r_2$ , leading to

$$E_2 = \begin{cases} E_1 & : 0 \leq r \leq r_1 \\ 0 & : r_1 < r \leq r_2 \end{cases} \quad (8)$$

$$H_2 = H_1 : 0 \leq r \leq r_1 . \quad (9)$$

Now only  $n_1$  eigenwaves in region 1 and  $n_2$  eigenwaves in region 2 are considered. The electric field in area 1 is expanded subject to the eigenfunctions in area 2 and the magnetic field in area 2 subject to the eigenfunctions in area 1. After some manipulations, in particular interchanging integrals and finite sums, the following relationship between voltage coefficients in region 1 and 2 can be formulated in matrix notation:

$$\begin{pmatrix} U_E^2 \\ U_H^2 \end{pmatrix} = \begin{pmatrix} X_{EE} & X_{HE} \\ X_{EH} & X_{HH} \end{pmatrix} \begin{pmatrix} U_E^1 \\ U_H^1 \end{pmatrix} . \quad (10)$$

Here  $U_E^k$  and  $U_H^k$  are vectors, consisting of the coefficients  $U_{E,j}^k$  and  $U_{H,j}^k$  for  $j = 1, \dots, n_k$ , respectively,  $k = 1, 2$ . The elements of the matrix  $X_{EE}$  are given by

$$X_{EE}^{ij} = \int_0^{r_2} \int_0^{2\pi} e_{E_i}^2(\rho, z, \phi)^T e_{E_j}^1(\rho, z, \phi) \rho d\phi d\rho . \quad (11)$$

In a similar way  $X_{HE}$ ,  $X_{EH}$ , and  $X_{HH}$  are defined. Moreover, very similar expressions for the current coefficients are available,

$$\begin{pmatrix} I_E^2 \\ I_H^2 \end{pmatrix} = \begin{pmatrix} Y_{EE} & Y_{HE} \\ Y_{EH} & Y_{HH} \end{pmatrix} \begin{pmatrix} I_E^1 \\ I_H^1 \end{pmatrix}, \quad (12)$$

where  $I_E^k$  and  $I_H^k$  are vectors, consisting of the coefficients  $I_{E,j}^k$  and  $I_{H,j}^k$  for  $j = 1, \dots, n_k$ , respectively,  $k = 1, 2$ .

Next the relationship between the mode amplitude vectors  $b_E^k$  and  $b_H^k$  of the excent waves  $b_{E,j}^k$ ,  $b_{H,j}^k$ , and  $a_E^k$  and  $a_H^k$  of the incident waves  $a_{E,j}^k$ ,  $a_{H,j}^k$ ,  $j = 1, \dots, n_k$ ,  $k = 1, 2$ , are evaluated. Proceeding from (7) and (10), (12), and the diagonal matrix

$$Z_k = \text{diag}(z_{E,1}^k, \dots, z_{E,n_k}^k, z_{H,1}^k, \dots, z_{H,n_k}^k), \quad (13)$$

see (7), some auxiliary matrices are defined:

$$\begin{aligned} A &= Z_2 - X Z_1^2 Y Z_2^{-1}, \\ B &= 2 X Z_1, \\ C &= -Z_2 - X Z_1^2 Y Z_2^{-1}, \\ D &= -Z_1 Y Z_2^{-1}, \\ E &= Z_1 Y Z_2^{-1}. \end{aligned} \quad (14)$$

Here  $X$  and  $Y$  are the matrices, composed of  $X_{EE}$ ,  $X_{EH}$ ,  $X_{HE}$ , and  $X_{HH}$ , see (10), and  $Y_{EE}$ ,  $Y_{EH}$ ,  $Y_{HE}$ , and  $Y_{HH}$ , see (12), respectively.

Finally, the scattering matrix is obtained,

$$\begin{pmatrix} b_1 \\ b_2 \end{pmatrix} = \underbrace{\begin{pmatrix} S_{11} & S_{12} \\ S_{21} & S_{22} \end{pmatrix}}_{\text{scattering matrix}} \begin{pmatrix} a_1 \\ a_2 \end{pmatrix} \quad (15)$$

by

$$\begin{aligned}
 S_{11} &= \mathbf{1} + EA^{-1}B, \\
 S_{12} &= A^{-1}B, \\
 S_{21} &= D + EA^{-1}C, \\
 S_{22} &= A^{-1}C,
 \end{aligned} \tag{16}$$

where  $\mathbf{1}$  is the  $2(n_1 + n_2)$ -dimensional identity matrix.

The next step is to combine scattering matrices of successive modules. First (15) is rewritten in the form

$$\begin{pmatrix} a_1 \\ b_1 \end{pmatrix} = \begin{pmatrix} T_{11} & T_{12} \\ T_{21} & T_{22} \end{pmatrix} \begin{pmatrix} a_2 \\ b_2 \end{pmatrix} \tag{17}$$

with

$$\begin{aligned}
 T_{11} &= S_{11}S_{21}^{-1}, \\
 T_{12} &= S_{12} - S_{11}S_{21}^{-1}S_{22}, \\
 T_{21} &= S_{21}^{-1}, \\
 T_{22} &= -S_{21}^{-1}S_{22}.
 \end{aligned} \tag{18}$$

In the same way, a transition matrix for the subsequent module is computed, say

$$\begin{pmatrix} \bar{a}_1 \\ \bar{b}_1 \end{pmatrix} = \begin{pmatrix} \bar{T}_{11} & \bar{T}_{12} \\ \bar{T}_{21} & \bar{T}_{22} \end{pmatrix} \begin{pmatrix} \bar{a}_2 \\ \bar{b}_2 \end{pmatrix}. \tag{19}$$

Since the input of the second module must coincide with the output of the first one, i.e.,  $\bar{a}_1 = b_2$  and  $\bar{b}_1 = a_2$ , it follows that

$$\begin{pmatrix} a_1 \\ b_1 \end{pmatrix} = \begin{pmatrix} T_{11} & T_{12} \\ T_{21} & T_{22} \end{pmatrix} \begin{pmatrix} \bar{T}_{21} & \bar{T}_{22} \\ \bar{T}_{11} & \bar{T}_{12} \end{pmatrix} \begin{pmatrix} \bar{a}_2 \\ \bar{b}_2 \end{pmatrix}. \tag{20}$$

A numerically more stable variant is proposed by Kühn and Hombach [15], which is also implemented for our numerical tests. By successive evaluation w.r.t. all horn

modules under consideration, we compute the total scattering matrix relating the amplitudes at the feed input with those at the aperture, i.e.,

$$\begin{pmatrix} b_1 \\ b_2 \end{pmatrix} = \underbrace{\begin{pmatrix} S_{11}^* & S_{12}^* \\ S_{21}^* & S_{22}^* \end{pmatrix}}_{\text{total scattering matrix}} \begin{pmatrix} a_1 \\ a_2 \end{pmatrix}. \quad (21)$$

## 5 The Optimization Model

First one has to determine the mode spectrum at the aperture from the far field, e.g. by the method of moments, see Hartwanger [12] for details. Proceeding from a given mode spectrum at the aperture, the next step is to compute the interior geometry of the horn to generate the required mode spectrum as closely as possible.

Optimization parameters are the geometric variables that determine the envelope functions, see Section 3, i.e.

$$p = (r_a, x_1, x_{con}, x_a, \alpha, l_r, l_s, t_1, t_2)^T$$

with

- $r_a$  - aperture radius,
- $x_1$  - length of input section,
- $x_{con}$  - length of conical section,
- $x_a$  - total horn length,
- $\alpha$  - semi flare angle of conical section,
- $l_r$  - width of slots,
- $l_s$  - width of ridges,
- $t_1$  - depth of first slot in input section,
- $t_2$  - depth of slots in conical section.

Some of these variables, especially the aperture radius, may be fixed during the optimization process depending on additional technical requirements. Proceeding from given initial values, the optimization algorithm approximates an optimal solution subject to some given termination tolerances.

From the analytical equations that determine the envelope functions, the corresponding diameters, widths of slots and ridges, etc. are determined, from which all data, needed for the successive evaluation of the scattering matrix (21), are computed. To illustrate the dependency of the scattering matrix from the geometric variables, (21) is reformulated to

$$\begin{pmatrix} b_1(p) \\ b_2(p) \end{pmatrix} = \underbrace{\begin{pmatrix} S_{11}^*(p) & S_{12}^*(p) \\ S_{21}^*(p) & S_{22}^*(p) \end{pmatrix}}_{\text{total scattering matrix}} \begin{pmatrix} a_1 \\ a_2 \end{pmatrix}. \quad (22)$$

The vector  $a_1$  describes the amplitudes of the modes exciting the horn, i.e. the  $TE_{11}$  mode in our case. Thus  $a_1$  is the  $2n_1$ -dimensional unity vector. The vector  $a_2$  is containing the amplitudes of the reflected modes at the horn aperture, known from the evaluation of the far field. Thus, a simple matrix time vector computation is performed to get the modes of reflected waves  $b_1(p)$  and  $b_2(p)$ , once the scattering matrix is known.

The main goal of the optimization procedure is to find an interior geometry  $p$  of the horn so that the distances of  $b_2(p)^j$  from given amplitudes  $\bar{b}_2^j$  for  $j = 1, \dots, 2n_2$  become as small as possible. The first component of the vector  $b_1(p)$  is a physically significant parameter, the so-called return loss, representing the power, reflected at the throat of the horn. Obviously, this return loss should be minimized as well. The phase of the return loss and further components of  $b_1(p)$  are not of interest.

From these considerations the least squares optimization problem

$$\begin{aligned} \min \sum_{j=1}^{2n_2} (b_2^j(p) - \bar{b}_2^j)^2 + \mu b_1^1(p)^2 \\ p \in \mathbb{R}^n : p_l \leq p \leq p_u \end{aligned} \quad (23)$$

is obtained. Here the upper index  $j$  denotes the  $j$ -th coefficient of the corresponding

vector,  $\mu$  a suitable weight, and  $p_l, p_u$  lower and upper bounds for the parameters to be optimized. Note also that complex numbers are evaluated throughout the paper. To get an implementable optimization problem, one has to consider real and imaginary part of objective function in (23) separately.

## 6 Solving Least Squares Problems

Besides of some very special cases, available optimization algorithms are unable to exploit the special structure of a data fitting formulation, i.e., that the norm of certain differences of a model function from given data points is to be minimized. The popular  $L_2$ -norm leads to a least squares problem of the form

$$\begin{aligned} \min & \sum_{i=1}^l f_i(p)^2 \\ p \in \mathbb{R}^n : & p_l \leq p \leq p_u \end{aligned} \quad , \quad (24)$$

cf. (23). Now it is assumed that the parameter vector  $p$  is  $n$ -dimensional and that all nonlinear functions are continuously differentiable with respect to  $p$ . Upper and lower bounds are taken into account. Further linear or nonlinear equality and inequality constraints can be included, but are omitted now to simplify the notation.

The assumption, that all problem functions must be smooth, is essential. The efficient numerical algorithm under consideration are based more or less on the Gauss-Newton method, that requires first derivatives. To understand their basic structure, the notation

$$F(p) := (f_1(p), \dots, f_l(p))^T$$

is introduced for the objective function vector, also called the residual. Moreover, let

$$f(p) := \frac{1}{2} \sum_{i=1}^l f_i(p)^2 \quad .$$

Then

$$\nabla f(p) = \nabla F(p)F(p) \quad (25)$$

defines the Jacobian of the objective function with

$$\nabla F(p) = (\nabla f_1(p), \dots, \nabla f_l(p)) .$$

If it is assumed now that the problem functions  $f_1, \dots, f_l$  are twice continuously differentiable, the Hessian matrix of  $f$  is given by

$$\nabla^2 f(p) = \nabla F(p) \nabla F(p)^T + B(p) , \quad (26)$$

where

$$B(p) := \sum_{i=1}^l f_i(p) \nabla^2 f_i(p) . \quad (27)$$

Proceeding from a given iterate  $p_k$ , Newton's method can be applied to (24) to get a search direction  $d_k \in \mathbb{R}^n$  by solving the linear system

$$\nabla^2 f(p_k) d + \nabla f(p_k) = 0$$

or alternatively,

$$\nabla F(p_k) \nabla F(p_k)^T d + B(p_k) d + \nabla F(p_k) F(p_k) = 0 . \quad (28)$$

Let us assume for a moment that

$$F(p^*) = (f_1(p^*), \dots, f_l(p^*))^T = 0$$

at an optimal solution  $p^*$ , i.e. that the residual  $F(p)$  vanishes at  $p^*$ . Then matrix  $B(p_k)$  in (28) is neglected, cf. (27) for justification, and (28) defines the normal equations of the linear least squares problem

$$\min_{d \in \mathbb{R}^n} \|\nabla F(p_k)^T d + F(p_k)\| . \quad (29)$$

A new iterate is obtained by  $p_{k+1} := p_k + \alpha_k d_k$ , where  $d_k$  is a solution of (29) and where  $\alpha_k$  denotes a suitable steplength parameter. It is obvious that a quadratic convergence rate is achieved when starting sufficiently close to an optimal solution. The above calculation of a search direction is known as the Gauß-Newton method and represents the traditional way to solve nonlinear least squares problems, see Björck [1] for more details.

In general, the Gauss-Newton method possesses the attractive feature that it converges quadratically to an optimal solution, although any second order information is not provided. Important assumptions are, that the Jacobian matrix of  $F$  possesses full rank and is Lipschitz continuous in a neighbourhood of  $p^*$ , and that the starting point  $p_0$  of the Gauss-Newton method with steplength one are sufficiently close to  $p^*$ . However, these assumptions are very strong and cannot be satisfied in real situations. There are problems with non-zero residuals, with rank-deficient Jacobian matrices, with non-continuous derivatives, and with starting points far away from a solution.

Especially difficulties arise when problems with a large residual are to be solved, i.e. if  $F(p^*)^T F(p^*)$  is not sufficiently small relative e.g. to  $\|\nabla F(p^*)\|$ . Numerous proposals have been made in the past to deal with this situation, and it is outside the scope of this paper to give a review on all possible attempts, developed in the last 20 years. Only a few remarks are presented to illustrate basic features of the main approaches, for further reviews see Gill, Murray, and Wright [10], Ramsin and Wedin [26] or Dennis [5].

A very popular method is known under the name Levenberg-Marquardt algorithm, see [16] and [19]. The key idea is to replace the Hessian in (28) by a multiple of the identity matrix, say  $\lambda_k I$ , with a suitable nonnegative factor  $\lambda_k$ . Obviously a regular system of linear equations of the form

$$\nabla F(p_k) \nabla F(p_k)^T d + \lambda_k d + \nabla F(p_k) F(p_k) = 0$$

follows. For the choice of  $\lambda_k$  and the relationship to the so-called *trust region methods*, see e.g. Moré [22].

A more sophisticated idea is to replace  $B(p_k)$  in (28) by any quasi-Newton matrix  $B_k$ , cf. e.g. Dennis [6]. But some additional safeguards are necessary to deal with indefinite matrices  $\nabla F(p_k) \nabla F(p_k)^T + B_k$  in order to get a descent direction. A modified algorithm was proposed by Gill and Murray [9], where  $B_k$  is either equal to  $B(p_k)$ , a second order approximation of  $B(p_k)$ , or a quasi-Newton matrix. In this case a diagonal matrix is added to  $\nabla F(p_k) \nabla F(p_k)^T + B_k$  to obtain a positive

definite matrix. Lindström [17] proposed a combination of a Gauß-Newton and a Newton method by using a certain subspace minimization.

If however, the residual is too large, then there is no possibility to exploit the special structure, and a general unconstrained minimization algorithm, e.g. a quasi-Newton method, can be applied as well.

A lot of efficient special purpose computer programs are available to solve unconstrained least squares problems, and there is no specific need to invent another implementation. However, there exists a very simple approach to combine the valuable properties of Gauss-Newton methods with that of sequential quadratic programming (SQP) algorithms in a very simple and straightforward way with nearly no additional efforts.

Since most nonlinear least squares problems are ill-conditioned, it is not recommended to solve (24) directly by a general nonlinear programming method. But a simple transformation of the original problem and its subsequent solution by an SQP method retains typical features of a special purpose code and prevents the need to take care of any negative eigenvalues of an approximated Hessian matrix. The corresponding computer program can be implemented in a few lines, provided that an SQP algorithm is available.

The transformation, also described in Schittkowski [28], is performed by introducing  $l$  additional variables  $z = (z_1, \dots, z_l)^T$  and  $l$  additional equality constraints of the form

$$f_i(p) - z_i = 0, \quad i = 1, \dots, l. \quad (30)$$

Then the equivalent transformed problem is

$$\begin{aligned} & \min \frac{1}{2} z^T z \\ & (p, z) \in \mathbb{R}^{n+l} : \quad F(p) - z = 0, \\ & \quad p_l \leq p \leq p_u. \end{aligned} \quad (31)$$

We consider now (31) as a general nonlinear programming problem of the form

$$\begin{aligned} & \min \bar{f}(\bar{p}) \\ & \bar{p} \in \mathbb{R}^{\bar{n}} : \bar{g}(\bar{p}) = 0, \\ & p_l \leq p \leq p_u \end{aligned} \tag{32}$$

with  $\bar{n} := n + l$ ,  $\bar{p} := (p, z)$ ,  $\bar{f}(\bar{p}) := \frac{1}{2}z^T z$ ,  $\bar{g}(\bar{p}) := F(p) - z$ , and apply the SQP method.

By transforming the original problem into a general nonlinear programming problem in the proposed way, typical features of a Gauss-Newton and quasi-Newton least squares method are retained, see Schittkowski [28] for details. The resulting optimization problem can be solved e.g. by a standard sequential quadratic programming code called NLPQL, cf. Schittkowski [27].

$$\bar{B}_k := \begin{pmatrix} B_k & 0 \\ 0 & I \end{pmatrix} \tag{33}$$

where  $B_k \in \mathbb{R}^{n \times n}$  denotes a suitable positive definite approximation of  $B(p)$ .

When starting the SQP method one could proceed from a user-provided initial guess  $p_0$  for the variables and define

$$\begin{aligned} z_0 &:= F(p_0), \\ B_0 &:= \begin{pmatrix} \epsilon I & 0 \\ 0 & I \end{pmatrix}, \end{aligned} \tag{34}$$

so that the initial point  $\bar{p}_0$  is feasible. The choice of  $B_0$  is of the form (33) and allows a user to provide some information on the estimated size of the residual, if available. If he knew that the residual  $F(p^*)^T F(p^*)$  is close to zero at the optimal solution  $p^*$ , he could choose a small  $\epsilon$  in (34). At least in the first iterates, the search directions are very similar to the traditional Gauß-Newton direction. Otherwise a user could define  $\epsilon = 1$ , if a large residual is expected.

## 7 Numerical Results

An existing *real-life* far field distribution is considered to illustrate the optimal design of a circular corrugated horn as described in the preceding sections. In the first step, the mode spectrum at the aperture is determined by the method of moments, see Figure 4. An excellent agreement between the two far fields w.r.t. amplitude and phase is observed. Until 60 degrees, the most important region for the design of the antenna under consideration, both curves coincide more or less.

In a second step, the optimization strategy discussed before, is applied to compute the interior geometry of the horn by approximating the known mode spectrum. The least squares problem was solved by the technique outlined in the previous section, see Schittkowski [28], where a solution of the constrained nonlinear programming problem was obtained by the sequential quadratic programming code NLPQL of Schittkowski [27].

The radius of the feeding wave guide, and the radius of the aperture are kept constant, i.e.,  $r_g = 11.28 \text{ mm}$  and  $r_a = 90.73 \text{ mm}$ , where 37 ridges and slots are assumed. Parameter names, initial values  $p_0$ , and optimal solution values  $p_{opt}$  are listed in Table 7. The parameters differ slightly from those shown in Section 3 and 5, respectively. The number of modes, needed to calculate the scattering matrix, is 70. Forward differences are used to evaluate numerical derivatives subject to a tolerance of  $1.0^{-7}$ , and  $\mu = 1$  was set for weighting the return loss.

The optimization code NLPQL produced the following output to inform about the progress of the iteration cycle. The first column contains objective function values, that are identical to our least squares fitting criterion only if the corresponding values for constraint violation vanish. The number of line search iterations and the steplength are one when approaching the solution, indicating the ideal case for an SQP method, i.e. convergence behaviour as expected from the theory. The last column shows the decrease of the optimality criterion until termination tolerance  $1.0^{-7}$  is reached, see Schittkowski [27] for a precise definition. For the last iterations the convergence speed is faster than linear, but still slower than quadratic. This

<i>name</i>	$p_0^i$	$p_{opt}^i$		<i>comment</i>
$x_1$	50.0	111.85	-	length of input section
$x_{con}$	50.0	0.00	-	length of conical section
$x_o$	50.0	47.00	-	length of output section
$\alpha$	28.0	29.00	-	semi flare angle of conical section
$q$	0.25	0.20	-	quotient of slot and ridge width
$t_1$	12.5	11.97	-	depth of first slot in input section
$t_2$	7.2	7.82	-	depth of slots in conical section

Table 1: Initial and optimal parameter values

superliner convergence speed is also verified by the available optimization theory because of the so-called BFGS quasi-Newton updates of matrices approximating the Langrangian function. Roundoff errors in evaluation of scattering matrices and, in particular, approximation errors in gradient calculations prevent a more accurate solution.

OUTPUT IN THE FOLLOWING ORDER:

IT - ITERATION NUMBER  
 F - OBJECTIVE FUNCTION VALUE  
 SCV - SUM OF CONSTRAINT VIOLATION  
 NA - NUMBER OF ACTIVE CONSTRAINTS  
 I - NUMBER OF LINE SEARCH ITERATIONS  
 ALPHA - STEPLENGTH PARAMETER  
 DELTA - ADDITIONAL VARIABLE TO PREVENT INCONSISTENCY  
 KT - KUHN-TUCKER OPTIMALITY CRITERION

IT	F	SCV	NA	I	ALPHA	DELTA	KT
1	.16795478D+01	.00D+00	37	0	.00D+00	.00D+00	.37D+00

2	.14476536D+01	.57D+00	37	1	.10D+01	.00D+00	.31D+01
3	.11909891D+01	.68D+00	37	2	.10D+00	.00D+00	.43D+01
4	.85038794D+00	.80D+00	37	2	.10D+00	.00D+00	.91D+00
5	.31779869D+00	.42D+00	37	1	.10D+01	.00D+00	.32D+00
6	.11781251D+00	.24D+00	37	1	.10D+01	.00D+00	.12D+00
7	.55760883D-01	.25D+00	37	1	.10D+01	.00D+00	.25D-01
..	.....	....	..	.	.....	.....	....
..	.....	....	..	.	.....	.....	....
47	.17468205D-02	.18D-02	37	1	.10D+01	.00D+00	.15D-04
48	.17434926D-02	.52D-04	37	1	.10D+01	.00D+00	.53D-05
49	.17397940D-02	.40D-02	37	1	.10D+01	.00D+00	.44D-04
50	.17219966D-02	.35D-03	37	1	.10D+01	.00D+00	.22D-05
51	.17225078D-02	.53D-06	37	1	.10D+01	.00D+00	.13D-07

In Figure 5 the far field of the horn computed by the optimization algorithm and the given far field can be compared. Obviously, the given one is approximated very well with a cross polar value below  $-42.19\text{ dB}$ . The reflection loss is better than  $30\text{ dB}$ , which is a satisfying value.

## 8 Conclusions

An efficient numerical approach to compute the optimal RF design of circular corrugated horns useful for industrial application is presented. The interior geometric structure of a horn is described by envelope functions, from which the actual diameters, slot and ridge depths and widths etc. are derived. The scattering matrix, relating the incident and excident modal field at horn throat and horn aperture is computed for the actual geometry and the obtained mode spectrum is compared to the objective mode spectrum.

The resulting least squares problem is established and the numerical optimization procedure, using the variables of the geometrical envelope function as optimization parameters, is outlined. Based on a *real life* far field, the practical feasibility of the approach is shown.

## References

- [1] Björck A. (1990): *Least Squares Methods*, Elsevier
- [2] Clarricoats P.J.B., Olver A.D. (1984): *Corrugated Horns for Microwave Antennas*, P. Peregrinus
- [3] Cocciali R., Pelosi G., Ravanelli R. (1997): *A mode matching-integral technique for the analysis and design of corrugated horns*, Report, La Recherche Aerospatiale
- [4] Collin R.E. (1991): *Field Theory of Guided Waves*, IEEE Press, New York
- [5] Dennis J.E.jr. (1977): *Nonlinear least squares*, in: *The State of the Art in Numerical Analysis*, D. Jacobs ed., Academic Press
- [6] Dennis J.E.jr. (1973): *Some computational techniques for the nonlinear least squares problem*, in: *Numerical Solution of Systems of Nonlinear Algebraic Equations*, G.D. Byrne, C.A. Hall eds., Academic Press
- [7] Dennis J.E.jr., Gay D.M., Welsch R.E. (1981): *Algorithm 573: NL2SOL-An adaptive nonlinear least-squares algorithm*, ACM Transactions on Mathematical Software, Vol. 7, No. 3, 369–383
- [8] Gentili G.G., Pelosi G., Ravanelli R. (1997): *Design and optimization of corrugated feeds: X-Horn software package*, IEEE Antennas and Propagation Magazine, Vol. 29, No. 5, 96–98
- [9] Gill P.E., Murray W. (1978): *Algorithms for the solution of the non-linear least-squares problem*, SIAM Journal on Numerical Analysis, Vol. 15, 977–992
- [10] Gill P.E., Murray W., Wright M.H. (1981): *Practical Optimization*, Academic Press
- [11] Harrington R.F. (1961): *Time-Harmonic Electromagnetic Fields*, McGraw Hill, New York

- [12] Hartwanger C. (1996): *Optimierung von Antennenhörnern im Satellitenbau*, Diploma Thesis, University of Bayreuth
- [13] Jackson J.D. (1981): *Klassische Elektrodynamik*, de Gruyter
- [14] Johnson R.C., Jasik H. (1984): *Antenna Engineering*, McGraw Hill, New York
- [15] Kühn E., Hombach V. (1983): *Computer-aided analysis of corrugated horns with axial or ring-loaded radial slots*, Report, Research Institute of the *Deutsche Bundespost*, Germany
- [16] Levenberg K. (1944): *A method for the solution of certain problems in least squares*, Quarterly Applied Mathematics, Vol. 2, 164–168
- [17] Lindström P. (1982): *A stabilized Gauß-Newton algorithm for unconstrained least squares problems*, Report UMINF-102.82, Institute of Information Processing, University of Umea, Umea, Sweden
- [18] Lindström P. (1983): *A general purpose algorithm for nonlinear least squares problems with nonlinear constraints*, Report UMINF-103.83, Institute of Information Processing, University of Umea, Umea, Sweden
- [19] Marquardt D. (1963): *An algorithm for least-squares estimation of nonlinear parameters*, SIAM Journal of Applied Mathematics, Vol. 11, 431–441
- [20] Mittra R. (1973): *Computer Techniques for Electromagnetics*, Pergamon Press, Oxford
- [21] Mittra R., Lee S.W. (1971): *Analytical Techniques in the Theory of Guided Waves*, Macmillan, Toronto
- [22] Moré J.J. (1977): *The Levenberg-Marquardt algorithm: implementation and theory*, in: Numerical Analysis, G. Watson ed., Lecture Notes in Mathematics, Vol. 630, Springer
- [23] Olver A.D., Xiang J. (1988): *Design of profiled corrugated horns*, IEEE Transactions on Antennas and Prop., Vol. 36, 936–940

- [24] Olver A.D. (1983): *Dual-depth corrugated horn design*, Proceedings of the 13th European Microwave Conference, Nürnberg, 879–884
- [25] Piefke G. (1977): *Feldtheorie III*, Bibliographisches Institut
- [26] Ramsin H., Wedin P.A. (1977): *A comparison of some algorithms for the nonlinear least squares problem*, Nordisk Tidstr. Informationsbehandling (BIT), Vol. 17, 72–90
- [27] Schittkowski K. (1985/86): *NLPQL: A FORTRAN subroutine solving constrained nonlinear programming problems*, Annals of Operations Research, Vol. 5, 485–500
- [28] Schittkowski K. (1988), Solving nonlinear least squares problems by a general purpose SQP-method, in: *Trends in Mathematical Optimization*, K.-H. Hoffmann, J.-B. Hiriart-Urruty, C. Lemarechal, J. Zowe eds., International Series of Numerical Mathematics, Vol. 84, Birkhäuser, 295–309.
- [29] Shee K.K., Smith W.T. (1997): *Optimizing multimode horn feed arrays for offset reflector antennas using a constrained minimization algorithm to reduce cross polarization*, IEEE Transactions on Antennas and Propagation, Vol. 45, No. 12, 1883–1885
- [30] Silver S. (1949): *Microwave Antenna Theory and Design*, McGraw Hill, New York
- [31] Unger H.-G. (1981): *Eltex Studentexte Elektronik: Elektromagnetische Theorie für die Hochfrequenztechnik, Teil I*, Hüthig
- [32] Waldron R.A. (1969): *Theory of Guided Electromagnetic Waves*, Van Nostand Reinhold Company, London
- [33] Wolf H., Sauerer B., Fasold D., Schlesinger V. (1994): *Computer aided optimization of circular corrugated horns*, Proceedings of the Progress in Electromagnetics Research Symposium, Noordwijk, The Netherlands

[34] Zuhrt H. (1953): *Elektromagnetische Strahlungsfelder*, Springer

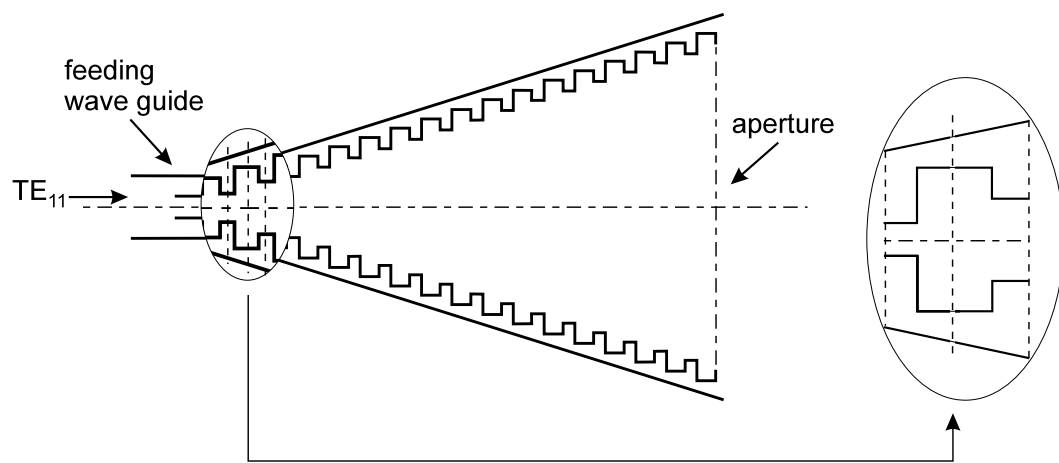


Figure 1: Cross sectional view of a circular corrugated horn

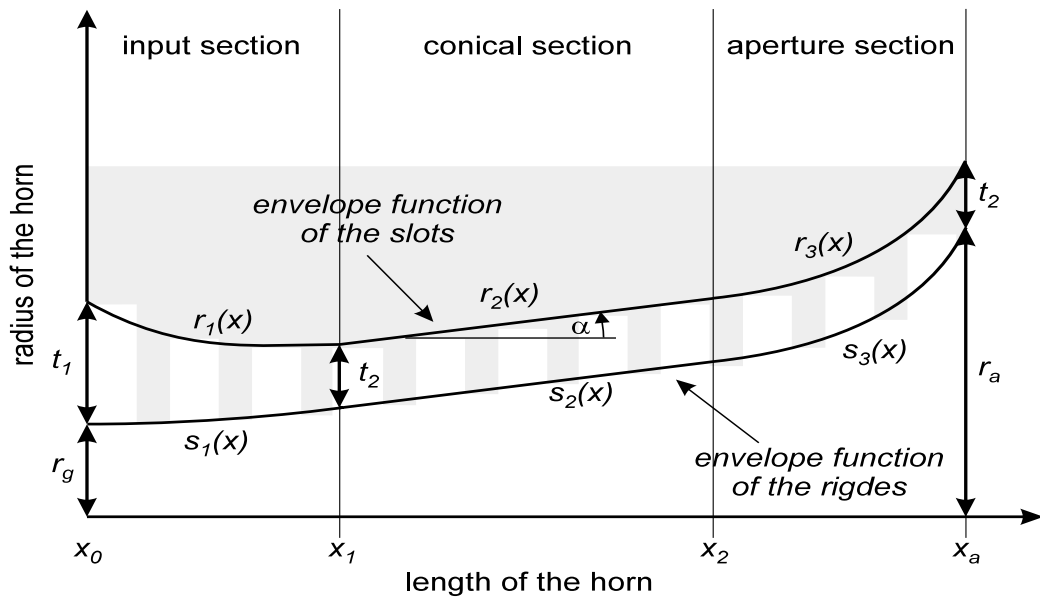


Figure 2: Envelope functions of a circular corrugated horn

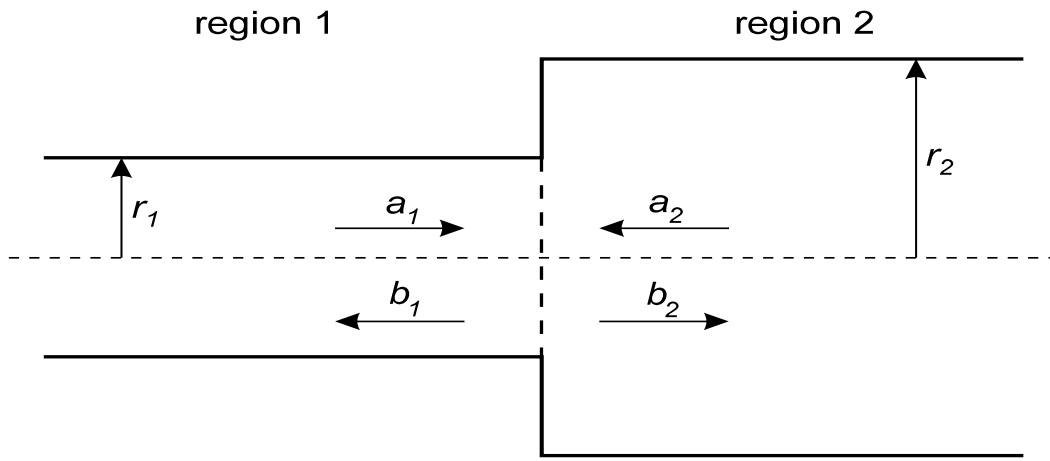


Figure 3: Cross sectional view of one module

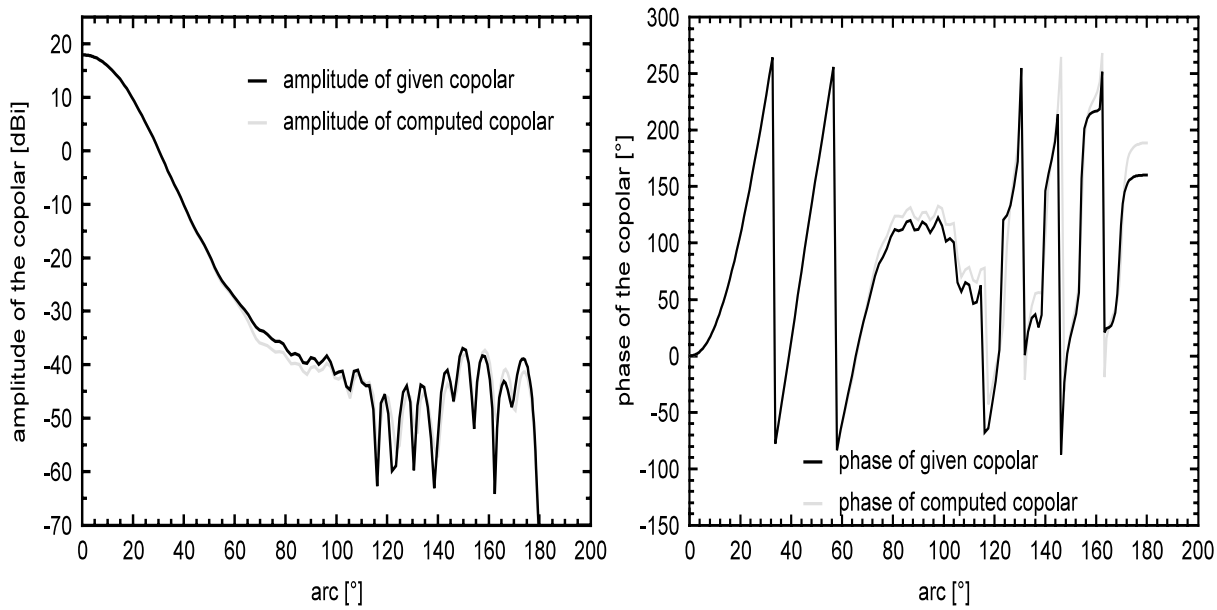


Figure 4: Amplitude and phase of copolar of given far field in comparison to the field excited by the computed aperture spectrum

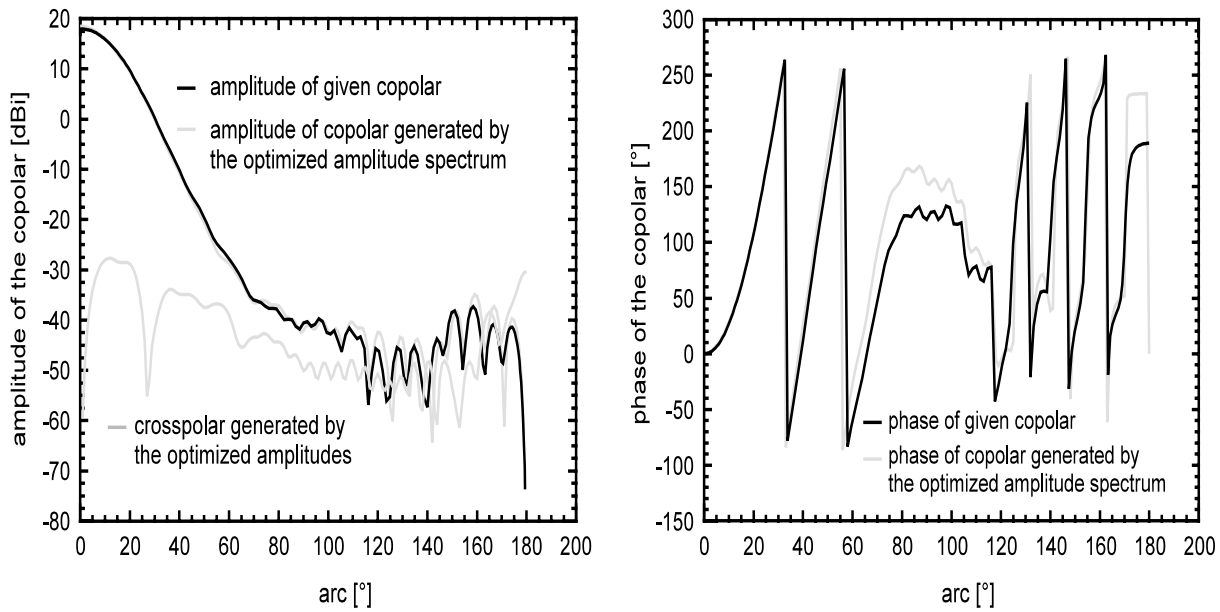


Figure 5: Comparison of far field of the optimised horn with the desired far field  
(left: magnitude, right: phase)

## List of Figures

1	Cross sectional view of a circular corrugated horn . . . . .	27
2	envelope function . . . . .	27
3	Cross sectional view of one module . . . . .	28
4	Amplitude and phase of copolar of given far field in comparison to the field excited by the computed aperture spectrum . . . . .	28
5	Comparison of far field of the optimised horn with the desired far field (left: magnitude, right: phase) . . . . .	29